Performance Comparison of MR-FDPF and Ray Launching in an Indoor Office Scenario

Xiaoming Tu*†‡, Hanye Hu*†‡, Zhihua Lai†, Jean-Marie Gorce* and Jie Zhang‡
*CITI Laboratory
INSA Lyon
Lyon, France
jean-marie.gorce@insa-lyon.fr
†Department of Research and Development
Ranplan Wireless Network Design Ltd.
Sheffield, UK
{xiaoming.tu, hanye.hu, zhihua.lai}@ranplan.co.uk
‡Department of Electronic and Electrical Engineering
University of Sheffield
Sheffield, UK
jie.zhang@sheffield.ac.uk

***Abstract*—Radio-wave propagation modelling plays a fundamental role in the wireless network planning and optimization. In this work, the performance of two propagation models which are based on different mechanisms are compared in an indoor office scenario in terms of speed and accuracy. Firstly, the office building is modelled and the properties of materials are tuned according to the measurement data so that they are more fit to the real environment. Then the two models are used to predict the coverage and the performance is analysed. Finally, a summary of the simulation results and the model recommendations are given.**

I. Introduction

With the fast development of radio networks and the heavy growth of mobile users, the QoS (Quality of Service) and capacity of a wireless network becomes much demanded than ever before. Network planning and optimization (P&O) tools, e.g. iBuildNet®[1] [1] from Ranplan Wireless Network Design Ltd., have been playing a important role in this area. They help the network designers to build stable and high quality networks before these networks are actually deployed, and thus reduce the costs those are raised from maintenance.

A satisfactory network P&O tool relies on accurate and fast radio propagation models. There are many propagation models that have been proposed in the literature. Those can be categorized into two kinds: empirical and deterministic models. Empirical models e.g. COST231 Multi-Wall [2], are computationally fast but they lack accuracy. The majority of empirical models do not consider the details of environments e.g. HATA model [3] which is based on the frequency and the distance between transmitters and receivers. Therefore, empirical models could be less effective for network P&O tools although the best advantage of network P&O tools is that they have detailed knowledge of the environment. On the contrary, deterministic models offer a high level of accuracy because they accounts for site-specific details such as building structures and materials. Currently, the most widely used deterministic models are FDTD-like models and ray optical methods [4].

In this work, two deterministic propagation models are compared: the MR-FDPF (Multi-Resolution Frequency Domain ParFlow) model [5] and the IRLA (Intelligent Ray Launching Algorithm) model [6]. MR-FDPF is based on the time domain ParFlow method, which solves the Maxwell's wave equation in time domain. By using a Fourier transform, it is possible to convert the local scattering matrix from the time domain to the frequency domain, thus solves the Maxwell's wave equation without a time boundary. IRLA is a ray launching based model which also employs the Geometrical Optics (GO) and the Geometrical Theory of Diffraction (GTD) [7]. Electromagnetic waves are modeled as rays that are launched from the signal source to the entire environment at discrete angles. At receiving locations, all rays arriving at different time delays are combined together by either being summed up or averaged to get the strength of the electric field.

This paper is organized as follows. In the next section, a brief introduction to the theory of the two propagation models is given. In Section III, an indoor environment which is used as the test bed for the comparison is described. The performance and analysis will be presented in Section IV. Finally, we will summarize the work and give the model recommendation that concludes this paper.

II. Model Description

A. MR-FDPF

The MR-FDPF model has been proven to be a fast and accurate way for predicting electric fields in indoor scenarios [8]. It is derived from the time domain ParFlow method and makes the method work in the frequency domain by a Fourier

[1] iBuildNet®is a trademark of Ranplan Wireless Network Design Ltd.

978-1-4799-0091-6/13/$31.00

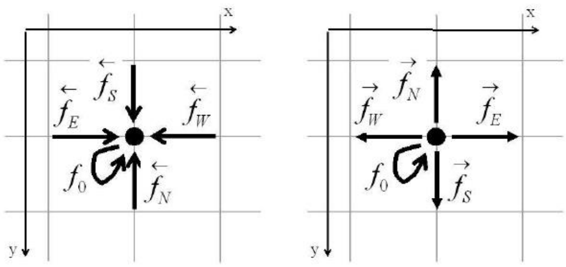

Fig. 1. First order approximation of wave equation on 2D grid

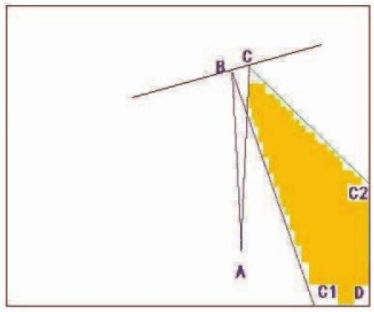

Fig. 2. Avoid ray dispersion

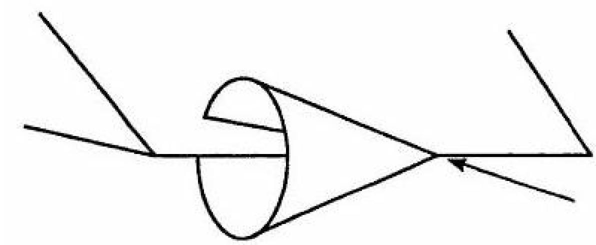

Fig. 3. Diffraction rays forms a 3D cone (Keller Cone)

transform of the local scattering matrix. Therefore, it is able to solve the wave equation without defining a time boundary.

The starting point of the MR-FDPF method is the Maxwell's wave equation in the time domain. It leads to the following equation after introducing a signal source:

$$\delta_t^2 \Psi(r,t) - (\frac{c_0}{n_r})^2 \cdot \delta_t^2 \Psi(r,t) = -\frac{1}{\epsilon} \cdot \delta_t i(r,t) \tag{1}$$

where $\Psi(r,t)$ is the electric field, $i(r,t)$ is the signal source and n_r is the refraction index of the media at location r. Constant c_0 is the speed of light. The time-domain ParFlow method is the first order approximation of (1) on the 2D grid as demonstrated in Fig. 1. The electric field is divided into four directional flows $f_d, d \in \{E,W,S,N\}$ and one stationary flow f_0 which is used to model different medium. Defining $\overleftarrow{F} = (\overleftarrow{f_E}, \overleftarrow{f_W}, \overleftarrow{f_S}, \overleftarrow{f_N}, f_0)^T$ and $\overrightarrow{F} = (\overrightarrow{f_E}, \overrightarrow{f_W}, \overrightarrow{f_S}, \overrightarrow{f_N}, f_0)^T$ for the inward the outward flows respectively, the approximation could be written as:

$$\overrightarrow{F}(r,t) = \Sigma(r) \cdot \overleftarrow{F}(r,t-dt) + \overrightarrow{S}(r,t) \tag{2}$$

where $\Sigma(r)$ is the local scattering matrix at pixel m: (i,j). Applying a Fourier Transform on equation (2), the problem is converted into the frequency domain leading to

$$\overrightarrow{F_e}(r) = \Sigma_e(r) \cdot \overleftarrow{F_e}(r) + \overrightarrow{S_e}(r) \tag{3}$$

where $\Sigma_e(r) = \Sigma(r) \cdot e^{-j2\pi v dt}$. Gathering all flows of each pixel, the propagation prediction over the entire environment is then converted into a linear inverse problem which can be modeled as the following mathematical equation:

$$(I_d - \Sigma_e)\overleftarrow{F_e} = \overrightarrow{S_e} \tag{4}$$

This linear inverse problem is then solved by matrix geometric series in MR-FDPF according to

$$\overleftarrow{F_e} = \sum_{k=0}^{\infty} (\Sigma_e)^k \cdot \overleftarrow{S_e} = \overleftarrow{S_e} + \Sigma_e \cdot \overleftarrow{S_e} + (\Sigma_e)^2 \cdot \overleftarrow{S_e} + \cdots \tag{5}$$

Finally, the electric field is computed directly by

$$\Psi(r, v_0) = \sum_{d=\{E,W,S,N\}} \overleftarrow{f_d}(r) \tag{6}$$

B. IRLA

The IRLA model is extended from the discrete ray launching mechanism which is widely used in Computer Graphics to model the light effect in 3D scenes. Rays are launched from the emitter and secondary rays that are caused by reflections or diffractions will be tracked when they hit the obstacles. These rays are sampled with a pre-defined angle aiming to cover the whole environment. However, rays will eventually disperse no matter how small the sampling angle is used after several reflections. Thus, some receiving points will be missed, especially for those distant receiving locations. There are many methods to avoid the problem, such as introducing an Impact Radius around a receiving point [9]; all rays those intersect with the reception sphere are considered as that they contribute to the total received signal on this receiver, or using the Tube-Launching method [9]. A new approach that is illustrated in Fig. 2 has been proposed to solve this problem for the IRLA model in [10]. When the rays reach a reflection face, all cubes between two reflected boundary rays will be filled by launching rays from each cube between B and C to each cube between C1 and C2 which are the hitting points of the reflected rays. In this approach, fewest rays are launched but all reflection area is covered. The calculation of intersections with receptions which is always time-consuming is not need anymore.

The GO theory itself does not take into account the shadowing effect, which however has significant impact on the radio wave propagations. Thus, the GTD is introduced to model the shadowing effect. In GTD, diffraction rays are modeled as a Keller Cone as illustrated in Fig. 3, where those rays form a 3D cone. The approach for avoiding ray dispersion effect is also applied to diffractions to fill the cubes in the cone.

Fig. 4. Floor plan of the indoor office building

III. Measurement Campaign

In order to compare the performance of these two propagation models, we have modeled an indoor office building in iBuildNet®. The calibration of materials' properties is mandatory in order to make simulation fit to the reality, i.e. tuning the material properties in the specific scenario.

A. Scenario

Fig. 4 illustrates the floor plan of the office building, which has a long corridor in the middle and dozens of rooms located on both side. The outside walls of the building are built up with concrete. Rooms are separated by walls with bricks. Doors and windows are made of wood and glass respectively. As shown in the figure, the transmitter is located in the middle of a room on the left side which is marked with a red text 'Tx'.

B. Measurement

The measurement data, which are received signal levels, are measured by using the equipment FSH spectrum analyzer [11]. The EIRP (Effective Isotropic Radiated Power) of the transmitter is set to 20dBm and the frequency is set to 3.4GHz to avoid potential interference from WiFi signal. The sensitivity of the analyzer is -141dBm/Hz, and the measured bandwidth is set to 300kHz. Thus the sensitivity in this case equals to $(-141 + 10\log(3 * 10^5)) \approx -86dBm$. To distinguish actual signals from noise, the signal levels measured above -86dBm are imported into iBuildNet®. Thus, 46 locations out of 70 measured locations were selected and they are employed to calibrate the two propagation models. Parameters of materials will be adjusted during the calibration process so that these parameters are more fit to the reality.

IV. Comparison

In this section, simulation results from the MR-FDPF model and the IRLA model are compared. Each of these models has been implemented as a dynamic link library (DLL) which is runnable in iBuildNet®. Before the comparison, a calibration process is carried out to adjust the properties of materials. Simulations are performed with new calibrated parameters. And then, the performance and accuracy are compared.

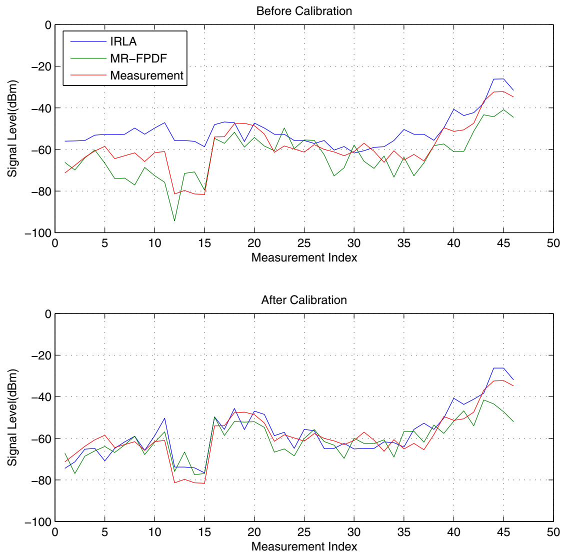

Fig. 5. Signal level comparison before and after calibration

A. Calibration

iBuildNet®has a material library which contains electromagnetical parameters of common materials however, these parameters have to be adjusted according to the specific scenario because the thickness or humidity of walls will influence them. Both these two models have its own calibration module for this purpose. They are carried out before predicting the coverage.

The MR-FDPF model employs the Genetic Algorithm (GA) [12] to process the calibration. The refraction index and attenuation coefficient of each material are grouped together as a chromosome (also known as a solution). In each generation of GA, dozens of chromosomes are randomly generated and the fitness of each solution, which is the root mean square errors (RMSE) between the prediction and measurement, is simultaneously calculated by multiple threads. Solutions with better fitness are selected to produce the next generation. The iteration ends when a number of iterations have been executed. The solution that has the best fitness is selected as the result of the calibration process. The IRLA implements a different approach to do the calibration, which is Simulate Annealing (SA) algorithm, but with the same fitness function as described above, i.e. RMSE.

Fig. 5 shows the calibration result for both models before and after the calibration. The RMSE is reduced from 10.46dB to 5.38dB for the MR-FDPF model, and from 7.83dB to 6.3dB for the IRLA model.

B. Performance

A set of signal level predictions is performed using two models separately at different resolutions, which are 0.1m,

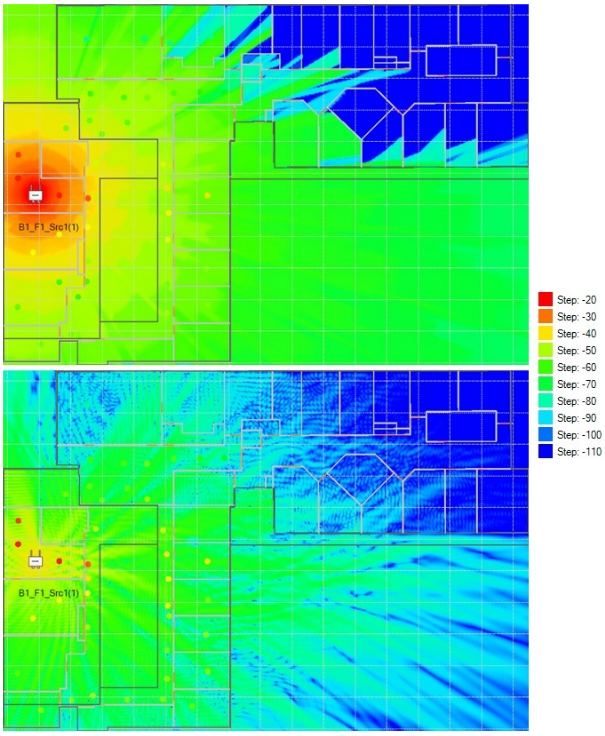

Fig. 6. Coverage comparison of IRLA(above) and MR-FDPF(below) with measurement points

TABLE I. COMPUTATION TIME AND MEMORY USAGE

	0.1m	0.2m	0.3m	0.5m
Time (IRLA)	9m44sec	43sec	8sec	3sec
Time (MR-FDPF)	38sec	8sec	4sec	2sec
Memory (IRLA)	1.02GB	205MB	94MB	42MB
Memory (MR-FDPF)	1.9GB	448MB	201MB	82MB

0.2m, 0.3m and 0.5m. The chosen resolution will have significant influence on the simulation speed and accuracy. The simulation result at 0.1m is shown in Fig. 6, in which the top plot is from IRLA model and the bottom plot is from MR-FDPF model. It should be noted that IRLA is configured to produce maximal 9 reflections, 9 transmissions and the limit of the path loss is restricted to 280dB which means a ray will be abandoned once the loss over its path exceeds this value.

Table. I lists the time and memory consumption of these two models at different resolutions. The calculation is performed on a laptop with Intel i7-3610QM CPU and 8GB RAM. In overall, the MR-FDPF model consumes less time but more memory than the IRLA model. The difference is significant especially when the resolution is set to 0.1m. It also should be noted that the IRLA performs 3D simulations but MR-FDPF only calculated in 2D.

C. Accuracy

The RMSEs of predictions compared with measurements at different resolutions are presented in Table. II. The accuracies of both models are similar, i.e. within 3dB, when the resolution is set no bigger than 0.3m, but the RMSE of MR-FDPF becomes large when the resolution is set to 0.5m. This is because that in the MR-FDPF model, the resolution is constrained by the wavelength. It is suggested to limit the resolution by one sixth of the wavelength, i.e. $\Delta_R \leq \lambda/6$ [5].

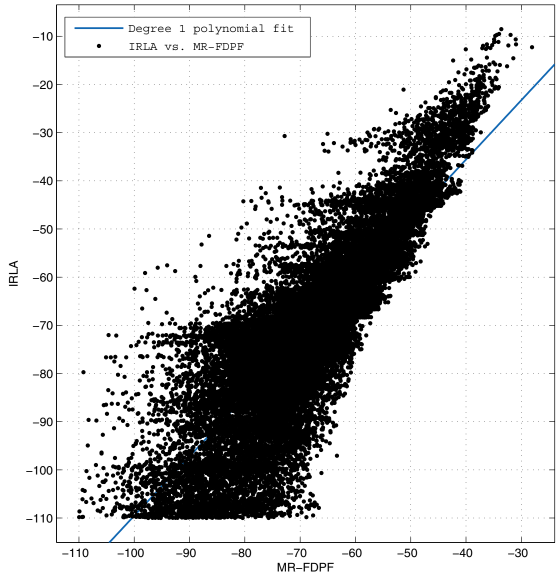

Fig. 7. Linear fit of prediction at 0.2m resolution

The Fig. 7 shows the best linear fitting for these two sets of predictions. The X axis represents the prediction from MR-FDPF and the Y axis represents the prediction from IRLA. The fitting polynomial with least RMSE is given as $f(x) = 1.232x + 13.71$. The function indicates that the IRLA tends to give an more optimistic prediction than MR-FDPF when the signal level is above $-59dBm$ while these values appear close to the signal source. And it can be seen form Fig.6 that the optimistic values from IRLA fit better with the measured values.

V. CONCLUSION

In this paper, we have given a brief introduction of the MR-FDPF model and the ray launching model, IRLA. Both have been used to predict the signal coverage in an indoor office scenario. Measurements are used to calibrate the materials' properties, which improves the prediction accuracy. The comparisons of two models have been presented and analyzed.

The presented prediction results from these two models are accurate and similar to each other at small resolutions. However at big resolution e.g. 5cm, the IRLA model still maintains accurate results, which is not the case for the MR-FDPF model. While in terms of the resource consumption, the MR-FDPF uses less time but more memory especially at small resolutions. It is worth noting that due to the nature of the MR-FDPF model, its performance is independent from the complexity of environments which however will increase the calculation load of the IRLA model by producing more reflections and transmissions.

TABLE II. ACCURACY

	0.1m	0.2m	0.3m	0.5m
RMSE (IRLA)	5.1dB	5.4dB	5.8dB	6.9dB
RMSE (MR-FDPF)	6.5dB	6.8dB	8.6dB	11.5dB

The comparison results indicate that both models are suitable for coverage predictions in indoor environments. Based on the comparison, it is recommended to use the MR-FDPF model for small or complex scenarios while for large scenarios, e.g. outdoors or very large buildings, the IRLA is more suitable.

ACKNOWLEDGMENT

This work is supported by the European FP7 iPlan project. The authors would like to thank the CITI laboratory, INSA-Lyon for providing the measurement data.

REFERENCES

[1] Ranplan Wireless Network Design, "iBuildNet: in-building wireless network planning and optimisation tool." [Online]. Available: http://www.ranplan.co.uk/ranplan-product/ibuildnet

[2] E. Damosso and CSELT, "Final Report for COST Action 231," Tech. Rep.

[3] M. Hata, "Empirical formula for propagation loss in land mobile radio services," *Vehicular Technology, IEEE Transactions on*, vol. 29, no. 3, pp. 317–325, Aug. 1980.

[4] M. Iskander, "Propagation prediction models for wireless communication systems," *Microwave Theory and Techniques, IEEE*, vol. 50, no. 3, pp. 662–673, 2002.

[5] J.-M. Gorce, K. Jaffres-Runser, and G. de la Roche, "Deterministic approach for fast simulations of indoor radio wave propagation," *Antennas and Propagation, IEEE Transactions on*, vol. 55, no. 3, pp. 938,948, 2007.

[6] Z. Lai, G. D. L. ROCHE, and N. Bessis, "Intelligent Ray Launching Algorithm for Indoor Scenarios," . . . , pp. 398–408, 2011.

[7] V. Borovikov and B. Kinber, "Geometrical theory of diffraction," *Journal of the Optical Society of America*, vol. 52, no. 2, pp. 116–130, 1962.

[8] G. Roche, K. Jaffres-Runser, and J. Gorce, "On predicting in-building WiFi coverage with a fast discrete approach," *International Journal of Mobile* . . . , vol. 2, pp. 3–12, 2007.

[9] S. Flores, L. Mayorgas, and F. Jimenez, "Reception algorithms for ray launching modeling of indoor propagation," in *Proceedings RAWCON 98. 1998 IEEE Radio and Wireless Conference (Cat. No.98EX194)*. IEEE, 1998, pp. 261–264.

[10] Z. Lai and N. Bessis, "A new approach to solve angular dispersion of discrete ray launching for urban scenarios," *. . . , 2009. LAPC 2009. . . .* , pp. 133–136, 2009.

[11] Rohde-Schwarz, "R&SFSH4 / R&SFSH8 / R&SFSH13 / R&SFSH20 Spectrum Analyzer - Rohde & Schwarz."

[12] M. Melanie, "An introduction to genetic algorithms," *Cambridge, Massachusetts London, England, Fifth printing*, vol. 3, 1999.